Catalysis Science & Technology

This article can be cited before page numbers have been issued, to do this please use: S. Iguchi, K. Teramura, S. Hosokawa and T. Tanaka, *Catal. Sci. Technol.*, 2016, DOI: 10.1039/C6CY00271D.

ROYAL SOCIETY OF CHEMISTRY

www.rsc.org/catalysis

View Article Online
DOI: 10.1039/C6CY00271D

Journal Name

ARTICLE

$ZnTa_2O_6$ photocatalyst synthesized via solid state reaction for conversion of CO_2 into CO in water †

Received 00th January 20xx,
Accepted 00th January 20xx

DOI: 10.1039/x0xx00000x

www.rsc.org/

Shoji Iguchi,[a] Kentaro Teramura,*[ab] Saburo Hosokawa,[ab] and Tsunehiro Tanaka*[ab]

Because of the environmental problems and the resulting exigent demand for CO_2 recycling processes, great attention is being paid to the photocatalytic conversion of CO_2 into useful chemicals such as CO, HCOOH, HCHO, CH_3OH, and CH_4. We have previously reported that the Ag-loaded, Zn-modified Ga_2O_3 photocatalyst exhibits excellent photocatalytic activity required for the conversion of CO_2 into CO by using H_2O as a reductant, and that the Ag particles that exist together with the Zn species act as good cocatalysts for the selective formation of CO. In this study, we demonstrated the photocatalytic activity of $ZnTa_2O_6$ under UV light irradiation, which was prepared via a solid-state reaction, for the conversion of CO_2 in an aqueous $NaHCO_3$ solution. Ag cocatalyst-loaded $ZnTa_2O_6$ photocatalyst evolved CO as a reduction product of CO_2 with 46% of the selectivity toward CO evolution among the reduction products. In contrast, when Pt and Au were introduced as cocatalysts, $ZnTa_2O_6$ photocatalyst evolved H_2 with high selectivity (> 99.9%).

Introduction

Artificial carbon cycling systems based on the catalytic conversion of CO_2 into useful carbon sources such as CO, HCOOH, HCHO, CH_3OH, and CH_4 are receiving a great deal of attention because of environmental issues such as global warming and natural resource depletion.[1–3] In heterogeneous catalysis, it is generally necessary to introduce a reducing reagent such as H_2 or a hydrocarbon at a high temperature in order to reduce CO_2.[3,4] However, H_2O is a more favorable reductant, because it is harmless and is an abundant source of protons. The photocatalytic conversion of CO_2 by means of H_2O, also known as artificial photosynthesis, is considered an uphill reaction involving photoexcited electrons and positive charge holes.[5,6] H_2 evolution via reduction of protons (H^+) takes place competitively during the photocatalytic conversion of CO_2 in water, because the standard reduction potential of CO_2 ($E°(CO_2/CO) = -0.11$ V vs. SHE)[7] is more negative than that of H^+ ($E°(H^+/H_2) = 0.0$ V vs. SHE).[7] In order to convert CO_2 to CO, rather than H_2 evolution from H^+, the photocatalyst surface should be design in such a way that it helps improve the selectivity of photogenerated electrons toward CO_2 reduction. The primary strategy for designing such a photocatalyst is to provide suitable surface properties to enable the absorption of CO_2.

We previously reported that ZrO_2,[8–11] MgO,[12,13] and Ga_2O_3,[14] which can act as solid base materials, were active for the photocatalytic conversion of CO_2 in the presence of H_2 as a reductant. Detailed analyses of the adsorbed species formed on the surface of these photocatalysts showed that the adsorption of a CO_2 molecule on the photocatalyst material is an essential step for the photocatalytic conversion of CO_2.[13,14] Moreover, the photocatalytic activities of layered double hydroxides (LDHs), which have high water-tolerant base sites, for the conversion of CO_2 in water were found.[15,16] In particular, the use of a Ni–Al LDH enables the selective evolution of CO as a reduction product of CO_2.[17] Another method for the selective conversion of CO_2 is the introduction of a metal cocatalyst onto the photocatalyst. Our research group also found that the Zn-modified Ga_2O_3 photocatalyst exhibited excellent activity for the conversion of CO_2 into CO and O_2 in the presence of Ag as a cocatalyst, with stoichiometric amounts of O_2 being formed as an oxidation product of H_2O.[18,19] We presume that Ag particles, in combination with the zinc species, can act as an effective cocatalyst for the conversion of CO_2 to CO, because the consumption of the photogenerated electrons by H^+ derived from H_2O was completely suppressed. These results indicate that a Ag cocatalyst in combination with a Zn-based mixed oxide semiconductor photocatalyst should enable the conversion of CO_2 with high selectivity under photoirradiation.

In this study we focused on the zinc tantalum mixed oxide as a photocatalyst for the conversion of CO_2 in water. A series of isostructural zinc tantalum mixed oxides: $ZnTa_2O_6$,[20–22] $Zn_3Ta_2O_8$,[23] and $Zn_4Ta_2O_9$,[24] have been successfully synthesized. Moreover, the photocatalytic activities of $ZnTa_2O_6$ [20] and $Zn_3Ta_2O_8$ [23] have been reported. Kato and Kudo (1998) showed the photocatalytic activity of $ZnTa_2O_6$ for water splitting in

---

[a] *Department of Molecular Engineering, Graduate School of Engineering, Kyoto University, Kyotodaigaku Katsura, Nishikyo-ku, Kyoto 615−8510, Japan. E-mail: teramura@moleng.kyoto-u.ac.jp (K.T.), tanakat@moleng.kyoto-u.ac.jp (T.T.); Fax: +81−75−383−2561; Tel: +81−75−383−2559*
[b] *Elements Strategy Initiative for Catalysts & Batteries (ESICB), Kyoto University, 1-30 Goryo-Ohara, Nishikyo-ku, Kyoto 615−8245, Japan.*

† Electronic Supplementary Information (ESI) available: See DOI: 10.1039/x0xx00000x

View Article Online
DOI: 10.1039/C6CY00271D

their summary of various tantalate photocatalysts; NiO-loaded $ZnTa_2O_6$ evolved H_2 at a rate of 15 μmol h^{-1} and O_2 at a rate of 6 μmol h^{-1} from distilled water under UV light irradiation.[25] As reviewed by Kudo et al., tantalum-based mixed oxides ($M_xTa_yO_z$) have excellent photocatalytic abilities, where M = Li, Na. K, Mg, Ca, Sr, Ba, Ni, Rb, or La, and showed stoichiometric decomposition of H_2O into H_2 and O_2 (H_2:O_2 = 2:1).[25] Takayama et al. reported that $KCaSrTa_5O_{15}$ photocatalyst, which shows good activity for the overall splitting of water using NiO as a cocatalyst, exhibited good activity for the reduction of CO_2 in water when Ag was loaded as a cocatalyst. [26] In contrast to the successful investigation of complete photocatalytic water splitting, the investigation on the photocatalytic conversion of CO_2 remains incomplete. In the present study, we demonstrate the photocatalytic activity of $ZnTa_2O_6$, synthesized via a solid-state reaction method, for the conversion of CO_2 to CO in an aqueous solution under UV irradiation.

Experimental Section

Catalyst preparation

$ZnTa_2O_6$ photocatalyst was prepared via a solid state reaction with referring the previous report.[22] The calculated amount of high purity Ta_2O_5 powder (Kojundo Chemical Laboratory) was added into an aqueous solution of $Zn(NO_3)_2 \cdot 6H_2O$ (Wako Pure Chemical) with molar ratio of Zn/Ta = 0.5. An aqueous NaOH solution was dropped to the suspension with vigorous stirring in order to adjust the pH at around 10.0–10.3, and then the resulting suspension was kept stable for 30 min at room temperature. The white suspension was aged at 363 K for 6 h with stirring by a magnetic stirrer. The resulting cake was collected by a vacuum filtration, and dried at room temperature under air condition. $ZnTa_2O_6$ was obtained through the calcination of this precursor for 12 h using an electric furnace at a specified temperature. $ZnTa_2O_6$ samples which were calcined at 1073, 1173, 1273, and 1373 K were hereinafter called ZTO_1073, ZTO_1173, ZTO_1273, and ZTO_1373, respectively. In addition, the polymerized complex method was used to synthesize $ZnTa_2O_6$. The required amount of $TaCl_5$ (Wako Pure Chemical) methanol solution and $Zn(NO_3)_2 \cdot 6H_2O$ (Wako Pure Chemical) were added into an aqueous citric acid solution, and stirred at room temperature. Ethylene glycol (Wako Pure Chemical) was added into this solution, and then stirred at 353 K to form a gelatinous solution. After the gel was heated at 723 K for 3 h with vigorous mixing, the resulting powder was calcined at 1273 K. $ZnTa_2O_6$ synthesized via the polymerized complex method would be presented as ZTO_PC. As a reference material, physical mixture of Ta_2O_5 and ZnO was prepared via a grinding of Ta_2O_5 and ZnO powder using an agate mortar, in advance, each of two powders was respectively calcined at 1273 K under an air atmosphere. One of the metal species (Ag, Au, Pt, Ni, and Cu) was loaded to the synthesized $ZnTa_2O_6$ as a cocatalyst for the photocatalytic reaction by impregnation, photodeposition, and chemical reduction methods. The cocatalyst loading procedures of these methods are described below based on the case of Ag. For the impregnation methods, an aqueous $AgNO_3$ solution including $ZnTa_2O_6$ powder was thoroughly evaporated at 353 K, and calcined at 723 K for 2 h in air. For the photodeposition method, $ZnTa_2O_6$ powder was dispersed in 1.0 L of ultra-pure water containing a required amount of $AgNO_3$, and the dissolved air in the solution was completely degassed by a flow of He gas. The suspension was irradiated under a 400 W high-pressure Hg lamp with a quartz filter using an inner-irradiation-type reaction vessel with He gas flowing. For the chemical reduction method, an aqueous solution of $NaPH_2O_2$ was added to a suspension of the $ZnTa_2O_6$ containing a given amount of $AgNO_3$. After stirring at 353 K for 2 h, the modified photocatalyst was filtered and washed with 1.0 L of ultra-pure water, and then dried at room temperature.

Catalyst characterization

X-ray diffraction (XRD) patterns of prepared samples were collected by using an X-ray diffractometer (Multi Flex, Rigaku), using Cu K_α radiation (λ = 0.154 nm) at a scan rate of 4 ° min^{-1}. Specific surface areas of the photocatalysts were estimated from their N_2 adsorption isotherms at 77 K using an adsorption analyzer (BELSORP-miniII, BEL Japan, Inc.). Prior to the measurements, each sample was evacuated at 673 K for 1 h using a pretreatment system (BELPREP-vacII, BEL Japan, Inc.). UV/Vis diffuse reflection spectra of synthesized materials were measured using a UV-Visible Spectrometer (V-650, JASCO) equipped with an integrated sphere accessory. Zn K-edge and Ta L_{III}-edge XAFS spectra of $ZnTa_2O_6$ were collected at the BL01B1 of SPring-8 with the approval of the Japan Synchrotron Radiation Research Institute (JASRI). The spectra were recorded in a transmittance mode at room temperature, using Si(111) double crystal monochromator. The photon energy was calibrated by using Zn foil. SEM images were captured using a Field Emission Scanning Electron Microscope (FE-SEM, SU-8220, Hitachi High-Technologies) at an acceleration voltage of 3.0 kV. FT-IR spectra of adsorbed species on a $ZnTa_2O_6$ were recorded with a FT-IR spectrometer (FT/IR-4000, JASCO) in a transmission mode at room temperature. A $ZnTa_2O_6$ sample (ca. 100 mg) was pressed into a wafer (diameter = 10 mm) and placed in an *in-situ* IR cell equipped with CaF_2 windows. The cell enabled to perform evacuation, heating, O_2 treatment, introduction of CO_2, and measurement of spectra in situ. Prior to measurement, the sample was evacuated at 673 K. followed by treatment with 5 kPa of O_2 for 1 h and evacuation for 15 min at 673 K. The background spectrum was obtained after the pretreatment at room temperature under evacuation. The data from 128 scans were accumulated at a resolution of 4 cm^{-1}.

Photocatalytic conversion of CO_2 in an aqueous solution

Photocatalytic reactions were performed by using an inner-irradiation type reactor vessel under a flow of CO_2 gas. 0.5 g of the photocatalyst powder was dispersed to 1.0 L of an ultra-pure water (if necessary, 0.1 M of $NaHCO_3$ was added to the

View Article Online
DOI: 10.1039/C6CY00271D

reaction solution as an additive), and the suspension was thoroughly degassed by a flow of CO_2 or He gas with a vigorous stirring. The reaction solution including a photocatalyst powder was illuminated by a 400 W high-pressure Hg lamp through a quartz glass jacket equipped with a water cooling system. Gas phase products were detected and quantified by using an online gas chromatograph (Tracera GC-2010plus, Shimadzu) equipped with a barrier discharge ionization detector (BID) using He gas as a carrier. The selectivity toward CO evolution among the reduction products was given by formula (1) as below,

Formula (1)

Selectivity toward CO evolution (%) = $100 \times \boldsymbol{R}_{CO} / (\boldsymbol{R}_{CO} + \boldsymbol{R}_{H2})$

where $\boldsymbol{R}_{CO}$ and $\boldsymbol{R}_{H2}$ was formation rates of CO and H_2, respectively.

For an isotopic experiment using ^{13}C-labeled CO_2 as a substrate, the photocatalytic reaction was conducted by using a closed circulation system connected to a rotary vacuum pump. 0.5 g of the photocatalyst powder was dispersed to 380 mL of an aqueous $NaHCO_3$ solution in the inner-irradiation type reaction vessel, and dissolved air in the reaction solution was degassed under a vacuum condition. 7.6 mmol of $^{13}CO_2$ (isotopic purity: 99 %, purchased from SI Science Co., Ltd.), which was purified by a freeze distillation, was introduced to the dead space. After the circulation for 30 min, the suspension was illuminated from an inner of the reaction vessel through the quartz filter by a 400 W high-pressure Hg lamp. A thermal conductivity detector gas chromatograph (GC-8A, Shimadzu) and a quadrupole mass spectrometer (BELMASS, MicrotracBEL) were used to detect the CO evolved in the gas phase.

Results and discussion

Figure 1 shows X-ray diffraction (XRD) patterns of $ZnTa_2O_6$ prepared via a solid-state reaction method; $ZnTa_2O_6$ was calcined at various temperatures. When compared to a reference pattern of $ZnTa_2O_6$ (Figure 1(d), ICSD #36289), our observations showed that $ZnTa_2O_6$ was successfully synthesized with no impurity phases, and that the diffraction peaks corresponding to ZnO (Figure 1(a)) and Ta_2O_5 (Figure 1(b)) were not found at all. No diffraction peaks corresponding to isostructural zinc tantalum mixed oxides such as $Zn_3Ta_2O_8$ and $Zn_4Ta_2O_9$ were observed in the XRD patterns of $ZnTa_2O_6$ (ZTO_1273, Figure 1(c)). In contrast to this, several impurity phases were observed in the XRD patterns of ZTO_1073 (Figure 1(e)) and ZTO_1173 (Figure 1(f)). In the case of ZTO_1173, a noticeably sharp diffraction peak was observed around 30°, confirming the formation of $ZnTa_2O_6$; in contrast, the XRD pattern of ZTO_1073 showed no clear peak in this region. These results indicate that the formation of the $ZnTa_2O_6$ starts at 1173 K and ends at 1273 K. As shown in Figure S1, the characteristic diffraction peaks assigned to the $ZnTa_2O_6$ structure appeared in the XRD patterns of ZTO_PC. Hence, the polymerized complex method resulted in poor crystallinity of ZTO_PC compared to ZTO_1273, which was prepared via a solid-state reaction.

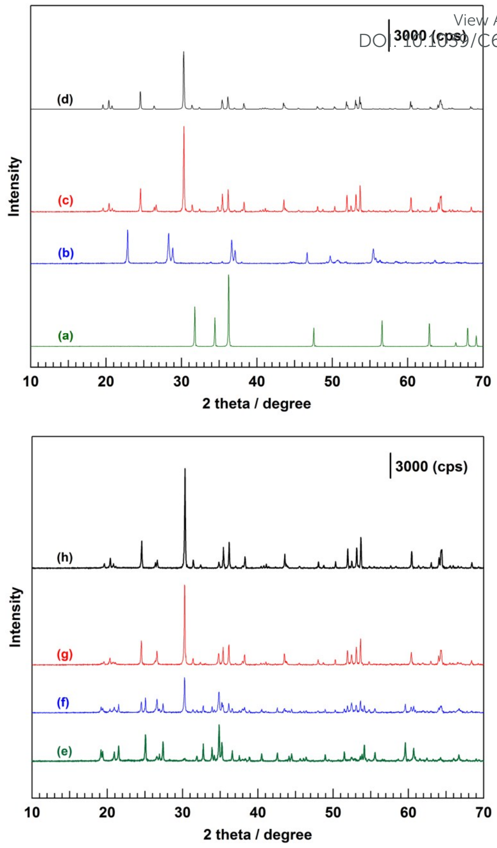

Fig. 1 XRD patterns of (a) ZnO, (b) Ta_2O_5, (c) and (g) ZTO_1273, (d) reference pattern of $ZnTa_2O_6$ (ICSD #36289), (e) ZTO_1073, (f) ZTO_1173, and (h) ZTO_1373.

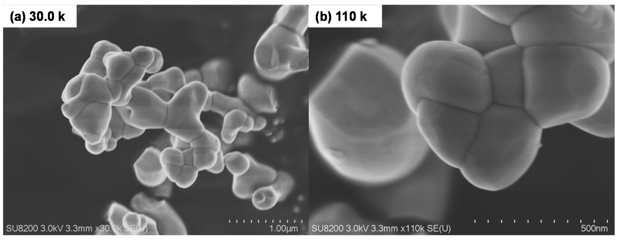

Fig. 2 SEM images of ZTO_1373 at magnification of (a) 30k and (b) 110k.

Figure 2 displays scanning electron microscopy images of ZTO_1373. The micrometer-sized particles were observed to have a very smooth surface, and were created by combining several submicron-sized particles with each other. Figure 3 shows UV/Vis diffuse reflectance spectra of $ZnTa_2O_6$ prepared at various temperatures and with different compositions of Ta_2O_5 and ZnO, as described in the experimental section. The results showed that an absorption edge of $ZnTa_2O_6$ was locates around 270 nm, whereas the absorption edge corresponding to Ta_2O_5 was found at 330 nm in the spectrum of the mixed sample. Based on the Davis-Mott equation [27] using the Kubelka-Munk function $\boldsymbol{F(R_\infty)}$ obtained from diffuse reflectance spectrum, the energy band gap of the $ZnTa_2O_6$ photocatalyst was estimated to be 4.5 eV.

View Article Online
DOI: 10.1039/C6CY00271D

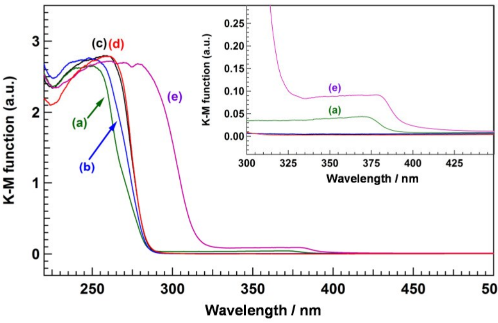

Fig. 3 UV/Vis diffuse reflectance spectra of (a) ZTO_1073, (b) ZTO_1173, (c) ZTO_1273, (d) ZTO_1373, and (e) mixture of ZnO + Ta_2O_5 (molar ratio Zn : Ta = 1 : 2). The inserting figure is enlarged view of small y-axis range.

Formula (2)

$$[\boldsymbol{F}(\boldsymbol{R}_\infty)\boldsymbol{hv}]^{-n} = \mathbf{A}(\boldsymbol{hv} - \boldsymbol{E_g})$$

where ***h***, ***v***, and **A** are Planck's constant, frequency of vibration, and proportional constant, respectively. The ZTO_1073 spectrum showed weaker absorption of ZnO than that of the mixture sample. The absorption peak of ZnO completely disappeared when the sample was calcined above 1173 K, indicating that the zinc species was completely conjugated with tantalum to form the $ZnTa_2O_6$ structure. Moreover, a broad absorption peak was observed in the spectra of the Ag-modified $ZnTa_2O_6$ samples, which can be ascribed to plasmonic absorption of Ag particles. As shown in Figure S2, Photoelectrochemical measurement also revealed that UV photoirradiation at wavelengths below 290 nm is necessary to induce the photocatalytic reaction over $ZnTa_2O_6$, because the anodic photocurrent was effectively diminished when a UV-29 long-pass filter is used.

Table 1 Formation rates of products evolved (H_2, O_2, and CO) and selectivity toward CO evolution in the photoacatalytic conversion of CO_2 in an aqueous $NaHCO_3$ solution. Photocatalyst powder: 0.5 g, volume of reaction solution: 1.0 L, additive: 0.1 M $NaHCO_3$, amount of cocatalyst loaded: 1 wt. %, atmosphere: CO_2 flow at a flow rate of 30 mL min^{-1}, light source: 400 W high-pressure Hg lamp.

Photocatalyst	[a] Formation rates of products / μmol h^{-1}			[b] Selectivity toward CO evolution (%)
	H_2	O_2	CO	
Bare ZTO_1273	19.7	9.3	6.6	25.1
[c] Pt/ZTO_1273	703.5	397.6	0.3	0.04
[c] Au/ZTO_1273	253.6	80.8	0.4	0.2
[c] Ni/ZTO_1273	135.0	67.6	0.2	0.1
[c] Cu/ZTO_1273	72.6	45.2	1.5	2.0
[d] Ag/ZTO_1273	25.1	18.6	19.3	43.4
[d] Ag/Ta_2O_5	6.5	3.3	2.1	24.4
[d, e] Ag/(ZnO + Ta_2O_5)	8.8	3.7	0.8	8.3
[d, f] Ag/ZTO_PC	14.7	4.2	2.4	13.8

[a] After 1 h of photoirradiation. [b] Calculated in accordance with equation (1). [c] Cocatalyst was loaded via photodeposition method. [d] Cocatalyst was loaded via impregnation method. [e] ZnO + Ta_2O_5: physical mixture. [f] ZTO_PC: synthesized via polymerized complex method.

Table 1 displays the formation rates of the products evolved (H_2, O_2, and CO) and the selectivity toward CO evolution during the photoacatalytic conversion of CO_2 in an aqueous $NaHCO_3$ solution using various metal-loaded ZTO_1273 and reference samples. Unmodified ZTO_1273 also exhibited photocatalytic activity under UV irradiation and generated reduction (H_2 and CO) and oxidation products (O_2). However, no photocatalytic activity was observed when the quartz jacket was replaced with a pyrex jacket. The photocatalytic activity was evidently influenced by modifying the $ZnTa_2O_6$ photocatalyst with a metal species as a cocatalyst. Loading of Pt, Au, Ni, and Cu cocatalysts enabled the splitting of water into H_2 and O_2 while simultaneously generating small amounts of CO as a reduction product of CO_2, indicating that H_2 evolution via a reduction of proton proceeded in preference to a reduction of CO_2. In particular, Pt/ZTO_1273, which was prepared via photodeposition method, showed fairly high overall water splitting activity and produced over 700 μmol of H_2 during 1 h of photoirradiation, whereas the formation rate of CO was only 0.3 μmol h^{-1}. In comparison, Ag-modified ZTO_1273 exhibited good activity for the conversion of CO_2 into CO. Although the total number of electrons consumed in the photocatalytic reaction was less than a tenth of Pt/ ZTO_1273, the formation rate of CO (19.3 μmol h^{-1}) was significantly higher than that of other cocatalyst. The selectivity toward CO evolution among the reduction products was 43.4% for the Ag/ZTO_1273 photocatalyst, whereas the percentage for ZTO_1273 modified with other cocatalysts was smaller by several percent points. The turnover number of electrons consumed for reduction of CO_2 into CO was 3.4 per Ag atom for 5 h of photoirradiation. Ag particle is considered to be an excellent cocatalyst for selective CO evolution in the photocatalytic conversion of CO_2, as it is recently known in the field of photocatalysis. Moreover, the formation rate of CO for ZTO_1273 was significantly higher than those for Ta_2O_5, ZTO_PC, and the physical mixture of ZnO and Ta_2O_5, indicating that the $ZnTa_2O_6$ photocatalyst, synthesized by the solid-state reaction, is more suitable for the conversion of CO_2 into CO in an aqueous $NaHCO_3$ solution under UV irradiation. The ratio of consumed electrons/holes in the photocatalytic reactions did not correspond to the stoichiometric value in the cases of Au/ZTO_1273 and Cu/ZTO_1273. It can be estimated that the counter anions of precursors of cocatalysts may cause undesired reactions under UV light irradiation. For example, chloride ions derived from $HAuCl_4$, which was used as a precursor of Au cocatalyst, should scavenge the photogenerated holes.

Figure 4 shows the amount of product evolved in the photocatalytic conversion of CO_2 in an aqueous $NaHCO_3$ solution using ZTO_1273 modified with Ag via impregnation (IMP), chemical reduction (CR), and photodeposition (PD) methods. The Ag-loading method affected both the photocatalytic activity and selectivity toward the evolution of CO. Ag/ZTO_1273, prepared via impregnation methods, exhibited the largest amount of CO evolved as a reduction product of CO_2. In comparison to previously developed compounds for the conversion of CO_2, the influence of the Ag-loading method on the photocatalytic activity and selectivity toward CO evolution was not as obvious; these compounds

View Article Online
DOI: 10.1039/C6CY00271D

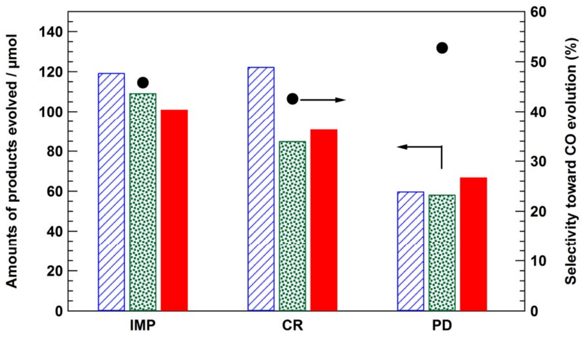

Fig. 4 Amount of products evolved in the photocatalytic conversion of CO_2 in an aqueous $NaHCO_3$ solution using ZTO_1273 photocatalyst modified with Ag via impregnation (IMP), chemical reduction (CR), and photodeposition (PD) methods. Photocatalyst powder: 0.5 g, volume of reaction solution: 1.0 L, additive: 0.1 M $NaHCO_3$, amount of Ag loaded: 3 wt. %, atmosphere: CO_2 flow at a flow rate of 30 mL min^{-1}, light source: 400 W high-pressure Hg lamp. Red (fill): CO, blue (slash): H_2, green (dot): O_2, and circle: selectivity toward CO evolution, reaction time: 5 h.

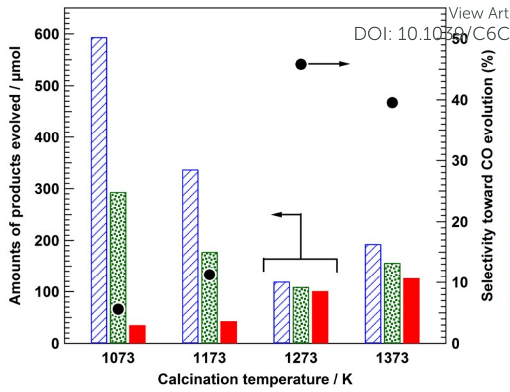

Fig. 5 Amounts of products evolved and the selectivity toward CO evolution in the photocatalytic conversion of CO_2 in an aqueous $NaHCO_3$ solution using ZTO_1073, ZTO_1173, ZTO_1273, and ZTO_1373 as photocatalysts. Photocatalyst powder: 0.5 g, volume of reaction solution: 1.0 L, additive: 0.1 M $NaHCO_3$, amount of Ag loaded: 3 wt. % (IMP), atmosphere: CO_2 flow at a flow rate of 30 mL min^{-1}, light source: 400 W high-pressure Hg lamp. Red (fill): CO, blue (slash): H_2, green (dot): O_2, and circle: selectivity toward CO evolution, reaction time: 5 h.

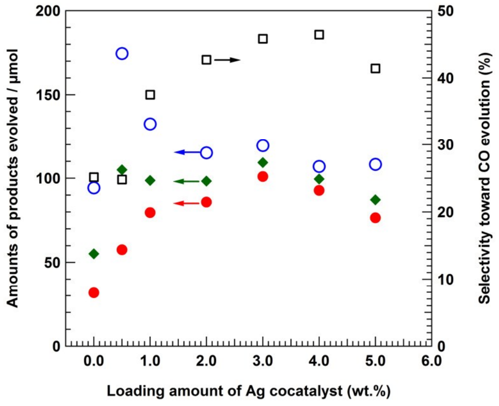

Fig. 6 Effect of Ag loading amount on the photocatalytic conversion of CO_2 in an aqueous $NaHCO_3$ solution using ZTO_1273 as a photocatalyst. Photocatalyst powder: 0.5 g, volume of reaction solution: 1.0 L, additive: 0.1 M $NaHCO_3$, Ag loading method: impregnation (IMP), atmosphere: CO_2 flow at a flow rate of 30 mL min^{-1}, light source: 400 W high-pressure Hg lamp. Red circle (fill): CO, blue circle (outlined): H_2, green diamond: O_2, and square: selectivity toward CO evolution, reaction time: 5 h.

include Zn-modified Ga_2O_3,[18,19] $ZnGa_2O_4$,[28] and SrO-modified Ta_2O_5 [29] reported by our group, and $BaLa_4Ti_4O_{15}$,[30] and $KCaSrTa_5O_{15}$ [26,31] reported by Kudo et al. After 5 h of photoirradiation, Ag/ZTO_1273, which was prepared by IMP, CR and PD methods, showed similar absorption peaks that corresponded to the plasmonic absorption of Ag in UV/Vis DR spectra. Thus, Ag/ZTO_1273 prepared via impregnation was used in the subsequent studies. As shown in Figure 5, the calcination temperature of the $ZnTa_2O_6$ photocatalyst drastically changed the photocatalytic activity for the conversion of CO_2 under UV irradiation. When $ZnTa_2O_6$ was synthesized through the calcination process at less than 1173 K (for ZTO_1073 and ZTO_1173), the main process was water splitting into H_2 and O_2. In contrast, only small amounts of CO were evolved as the reduction product of CO_2. Here, the selectivity toward CO evolution among the various reduction products was equal to or less than 10%. However, the photocatalytic activity changed at 1273 K, at which the selectivity toward CO evolution greatly increased to ca. 40% because H_2 generation via reduction of H^+ was effectively suppressed at 1273 K. The specific surface area (S_{BET}) of as synthesized $ZnTa_2O_6$ gradually decreased with the increase in the calcination temperature; specifically, when $ZnTa_2O_6$ was calcined at 1073, 1173, 1273, and 1373 K, the S_{BET} values became 2.5, 2.1, 1.8, and 1.4 m^2 g^{-1}, respectively. It is estimated that the decrease in the surface area of $ZnTa_2O_6$ is one of the reasons why the total number of consumed electrons in the photocatalytic reaction noticeably decreased at high calcination temperatures. Furthermore, the Zn-K edge XANES spectra of $ZnTa_2O_6$ materials showed that the structure was altered by the calcination temperature, as shown in Figure S3(a–e). Compared to the spectrum of the mixture sample (ZnO + Ta_2O_5), which shows the characteristic Zn^{2+} peak in ZnO, the Zn species in ZTO_1073 was different from ZnO; if anything, it should be similar to a four-fold coordination of Zn^{2+}, just like ZnS.[32] It is known that $Zn_3Ta_2O_8$ phase contains tetrahedral coordination of Zn^{2+}.[33] The XANES spectra of ZTO_1273 and ZTO_1373 were different from that of ZTO_1073, because the crystal structure of $ZnTa_2O_6$ is classified as a α-PbO_2 structure, in which Zn^{2+} species are in a six-fold coordination.[34] This result indicates that Zn species in the precursor should be transformed to six-fold coordination in order to construct the $ZnTa_2O_6$ structure via $Zn_3Ta_2O_8$ phase during the calcination above 1273 K. Therefore, the Zn-K edge XANES spectrum of ZTO_1173 was found to be between those of ZTO_1073 and ZTO_1273. As shown in Figure S3(f–j), in contrast, the XANES spectra of the Ta-L_{III} edge did not change on increasing the calcination temperature. Hence, we can conclude that based on the results of XRD and XAFS, the improvement in the selectivity toward CO evolution was due to the structural change of Zn species, which in the ZnO phase were incorporated into Ta_2O_5 to form a $ZnTa_2O_6$ structure when calcined above 1273 K, and because the potential of the photogenerated electrons in the conduction band of ZnO was

View Article Online
DOI: 10.1039/C6CY00271D

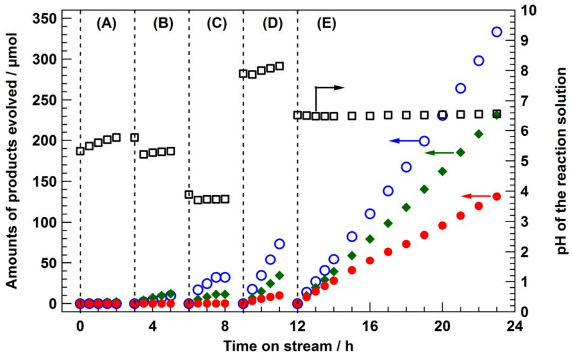

Fig. 7 Result of control experiments for the photocatalytic conversion of CO_2 using in water Ag/ZTO_1273 as a photocatalyst. (A) no additive; He gas flow; dark, (B) no additive; He gas flow; photoirradiation, (C) no additive; CO_2 gas flow; photoirradiation, (D) 0.1 M $NaHCO_3$ additive; He gas flow; photoirradiation, (E) 0.1 M $NaHCO_3$ additive; CO_2 gas flow; photoirradiation. Photocatalyst powder: 0.5 g, volume of reaction solution: 1.0 L, Ag loading: 3 wt. % (IMP), flow rate of gas: 30 mL min^{-1}, light source: 400 W high-pressure Hg lamp. Red circle (fill): CO, blue circle (outlined): H_2, green diamond: O_2, and square: pH of the reaction solution.

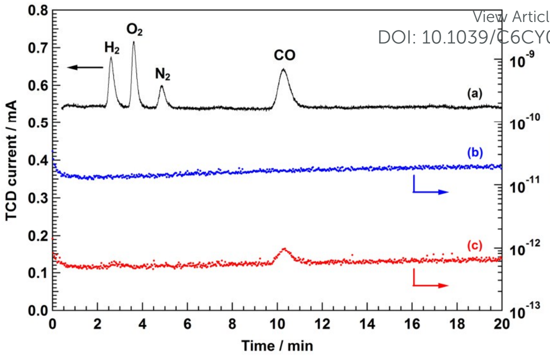

Fig. 8 GC-MS profile in the isotopic experiment for the photocatalytic conversion of ^{13}C-labeled CO_2 using ZTO_1273 as a photocatalyst. (a) TCD-GC chromatogram, Q-Mass profile of (b) m/z = 28, and (c) m/z = 29. Photocatalyst powder: 0.5 g, volume of reaction solution: 380 mL, additive: 0.1 M $NaHCO_3$, Ag loading: 3 wt. % (IMP), ^{13}C-labeled CO_2: 7.6 mmol, light source: 400 W high-pressure Hg lamp.

not enough to reduce CO_2.[35] The *in situ* FT-IR spectra of CO_2 adsorbed species on ZTO_1173 and ZTO_1273 are presented in Figure S4. Both of them showed absorption peaks corresponding to the C-O stretching of the CO_2 species adsorbed on the metal oxide materials, with reference to the review about the CO_2 species adsorbed on other simple metal oxides; [36] in contrast, it is difficult to determine the adsorbed CO_2 on the surface of Ta_2O_5. The absorption peaks observed at 1320, 1375, and 1632 cm^{-1} for both ZTO_1173 and ZTO_1273 can be assigned to the carbonate species.[36] The peaks at 1450 and 1730 cm^{-1} corresponding to bicarbonate species [36] were found in ZTO_1273, indicating that the surface properties of $ZnTa_2O_6$ were altered on changing the calcination temperature. Hence, it can be considered that changes in the chemical properties, which alter the adsorbed CO_2 species, improve the selectivity toward CO evolution.

Figure 6 displays the effect of the loading amount of Ag on the photocatalytic activity for the conversion of CO_2 in an aqueous $NaHCO_3$ solution using ZTO_1273 as a photocatalyst. As the loading amount of Ag was increased to 3.0 wt.%, the amount of CO evolved also increased, which was accompanied with a decrease in H_2 evolution. This is an indication that the selectivity toward CO evolution clearly improved on increasing the loading amount of Ag. As mentioned above, Ag particles loaded on a $ZnTa_2O_6$ photocatalyst are considered to be effective cocatalysts for the conversion of CO_2 into CO.

The results of the control experiments using Ag-loaded ZTO_1273 are presented in Figure 7. At region (A), no photocatalytic reaction was observed under dark condition under He gas flow. Small amounts of H_2 and O_2 were produced in the He atmosphere under UV irradiation, as shown in region (B). At region (C), small amounts of H_2 and O_2 were evolved from pure water under photoirradiation and CO_2 gas flow,. Prior to starting the region (D), $NaHCO_3$ (0.1 M) was added into the reaction solution and the dissolved air was completely degassed by the He gas flow. During illumination, small amounts of H_2, O_2, and CO were formed in the gas phase stoichiometrically. The selectivity toward CO evolution was ca. 10% in region (D), indicating that the main photocatalytic process was water splitting, which was accompanied by the conversion of $NaHCO_3$-derived CO_2. With the start of CO_2 gas flow in region (E), the evolution of CO noticeably improved. Moreover, the selectivity toward CO evolution was over 40% after 2 h of photoirradiation. The formation rate of CO gradually decreased with the irradiation duration, whereas that of H_2 remained stable during the 12 h of photoirradiation. It can be estimated that changes of Ag particles, such as particle size and oxidation state, caused the deterioration of the activity for CO evolution. Furthermore, the isotopic experiment was performed using ^{13}C-labeled CO_2 in order to confirm that carbon source of CO evolved in the photocatalytic conversion of CO_2 over Ag-modified ZTO_1273. Figure 8 shows the result of GC-MS analysis for the isotopic experiment. In the TCD-GC chromatogram, the clear peak at 10.5 min was assigned to CO, and the others peaks corresponded to H_2, O_2, and contaminated N_2. With a Q-Mass profile of m/z = 29, one peak was found at the same retention time to CO in the GC chromatogram, indicating that this peak can be considered to originate from the ^{13}C-labeled CO. In contrast, no peak was observed in the profile of m/z = 28. Hence, it can be concluded that the CO evolved in this study originated from CO_2. Therefore, other carbon sources such as the contamination of organic residues did not influence this photocatalytic reaction. Further investigation on the synthesis procedure of photocatalyst and cocatalyst modification is necessary, because the photocatalytic activity and selectivity toward CO evolution have not been insufficiently investigated. We found that the $ZnTa_2O_6$ photocatalyst is active for the conversion of CO_2 into CO under UV irradiation. The formation of stoichiometric amounts of O_2 indicates that H_2O can act both as an electron donor and a proton source for this reaction.

Conclusions

We found that the Ag cocatalyst-loaded $ZnTa_2O_6$ photocatalyst showed activity for the conversion of CO_2 into CO in an aqueous $NaHCO_3$ solution under UV irradiation. After 5 h of photoirradiation of Ag-loaded ZTO_1273 (3 wt.%), the amount of CO evolved was 109.3 μmol and the selectivity toward CO evolution among the reduction products was 45.8%. The formation of stoichiometric amounts of O_2 indicates that H_2O can act both as an electron donor and a proton source for this reaction. In contrast, Pt/ZTO_1273, which was prepared by the photodeposition method, showed good overall water splitting capabilities and over 700 μmol of H_2 was produced over 1 h of photoirradiation. Through control and isotopic experiments, we concluded that CO evolved during the photocatalytic conversion of CO_2 in an aqueous $NaHCO_3$ solution using the Ag cocatalyst-loaded $ZnTa_2O_6$ photocatalyst originated from the CO_2 introduced as a substrate. Calcination at high temperatures altered both the chemical and structural properties of $ZnTa_2O_6$ and improved the selectivity toward CO evolution.

Acknowledgements

This study was partially supported by a Grant-in-Aid for Scientific Research on Innovative Areas "All Nippon Artificial Photosynthesis Project for Living Earth" (No. 2406) of the Ministry of Education, Culture, Sports, Science, and Technology (MEXT) of Japan, the Precursory Research for Embryonic Science and Technology (PRESTO), supported by the Japan Science and Technology Agency (JST), and the Program for Element Strategy Initiative for Catalysts & Batteries (ESICB), commissioned by the MEXT of Japan. Shoji Iguchi thanks the JSPS Research Fellowships for Young Scientists.

References

1 W. Wang, S. Wang, X. Ma and J. Gong, *Chem. Soc. Revi.*, 2011, **40**, 3703-3727.
2 G. Centi, E. A. Quadrelli and S. Perathoner, *Energy Environ. Sci.*, 2013, **6**, 1711-1731.
3 E. V. Kondratenko, G. Mul, J. Baltrusaitis, G. O. Larrazabal and J. Perez-Ramirez, *Energy Environ. Sci.*, 2013, **6**, 3112-3135.
4 M.-S. Fan, A. Z. Abdullah and S. Bhatia, *ChemCatChem*, 2009, **1**, 192-208.
5 A. Kubacka, M. Fernández-García and G. Colón, *Chem. Rev.*, 2012, **112**, 1555-1614.
6 W. Fan, Q. Zhang and Y. Wang, *Phys. Chem. Chem. Phys.*, 2013, **15**, 2632-2649.
7 *Standard Potentials in Aqueous Solution*, Marcel Dekker, 1985.
8 Y. Kohno, T. Tanaka, T. Funabiki and S. Yoshida, *Chem. Commun.*, **1997**, 841-842.
9 Y. Kohno, T. Tanaka, T. Funabiki and S. Yoshida, *Chem. Lett.*, 1997, **26**, 993-994.
10 Y. Kohno, T. Tanaka, T. Funabiki and S. Yoshida, *J. Chem. Soc., Faraday Trans.*, 1998, **94**, 1875-1880.
11 Y. Kohno, T. Tanaka, T. Funabiki and S. Yoshida, *Phys. Chem. Chem. Phys.*, 2000, **2**, 2635-2639.
12 Y. Kohno, H. Ishikawa, T. Tanaka, T. Funabiki and S. Yoshida, *Phys. Chem. Chem. Phys.*, 2001, **3**, 1108-1113.
13 K. Teramura, T. Tanaka, H. Ishikawa, Y. Kohno and T. Funabiki, *J. Phys. Chem. B*, 2004, **108**, 346-354.
14 H. Tsuneoka, K. Teramura, T. Shishido and T. Tanaka, *J. Phys. Chem. C*, 2010, **114**, 8892-8898.
15 K. Teramura, S. Iguchi, Y. Mizuno, T. Shishido and T. Tanaka, *Angew. Chem. Int. Ed.*, 2012, **51**, 8008-8011.
16 S. Iguchi, K. Teramura, S. Hosokawa and T. Tanaka, *Catal. Today*, 2015, **251**, 140-144.
17 S. Iguchi, K. Teramura, S. Hosokawa and T. Tanaka, *Phys. Chem. Chem. Phys.*, 2015, **17**, 17995-18003.
18 K. Teramura, Z. Wang, S. Hosokawa, Y. Sakata and T. Tanaka, *Chem. A Euro. J.*, 2014, **20**, 9906-9909.
19 Z. Wang, K. Teramura, Z. Huang, S. Hosokawa, Y. Sakata and T. Tanaka, *Catal. Sci. Technol.*, 2015, DOI: 10.1039/C5CY01280E.
20 Z. Ding, W. Wu, S. Liang, H. Zheng and L. Wu, *Mater. Lett.*, 2011, **65**, 1598-1600.
21 G. B. Kunshina, I. V. Bocharova, O. G. Gromov, E. P. Lokshin and V. T. Kalinnikov, *Inorg. Mater.*, 2012, **48**, 62-66.
22 A. V. B. M. Birdeanu, E. Fagadar-Cosma, C. Enache, I. Miron, I. Grozescu, *Dig. J. Nanomater. Bios.*, 2013, **8**, 263-272.
23 T. H. Noh, I.-S. Cho, S. Lee, D. W. Kim, S. Park, S. W. Seo, C. W. Lee and K. S. Hong, *J. Am. Ceram. Soc.*, 2012, **95**, 227-231.
24 M. Waburg and H. Müller-Buschbaum, *Z. anorg. allg. Chem.*, 1985, **522**, 137-144.
25 H. Kato and A. Kudo, *Chemical Phys. Lett.*, 1998, **295**, 487-492.
26 T. Takayama, K. Tanabe, K. Saito, A. Iwase and A. Kudo, *Phys. Chem. Chem. Phys.*, 2014, **16**, 24417-24422.
27 E. A. Davis and N. F. Mott, *Philos. Mag.*, 1970, **22**, 0903-0922.
28 Z. Wang, K. Teramura, S. Hosokawa and T. Tanaka, *J. Mater. Chem. A*, 2015, **3**, 11313-11319.
29 K. Teramura, H. Tatsumi, Z. Wang, S. Hosokawa and T. Tanaka, *Bull. Chem. Soc. Jpn.*, 2015, **88**, 431-437.
30 K. Iizuka, T. Wato, Y. Miseki, K. Saito and A. Kudo, *J. Am. Chem. Soc.*, 2011, **133**, 20863-20868.
31 T. Takayama, A. Iwase and A. Kudo, *Bull. Chem. Soc. Jpn.*, 2015, **88**, 538-543.
32 R. Kretzschmar, T. Mansfeldt, P. N. Mandaliev, K. Barmettler, M. A. Marcus and A. Voegelin, *Environ. Sci. Technol.*, 2012, **46**, 12381-12390.
33 S. K. Kurinec, P. D. Rack, M. D. Potter, and T. N. Blanton, *J. Mater. Res.*, 2000, **15**, 1320-1323.
34 M. Waburg and H. Müller-Buschbaum, *Z. anorg. allg. Chem.*, 1984, **508**, 55-60.
35 G. Busca and V. Lorenzelli, *Mater. Chem.*, 1982, **7**, 89-126.
36 T. Stimpfling and F. Leroux, *Chem. Mater.*, 2010, **22**, 974-987.

View Article Online
DOI: 10.1039/C6CY00271D

Graphical abstract

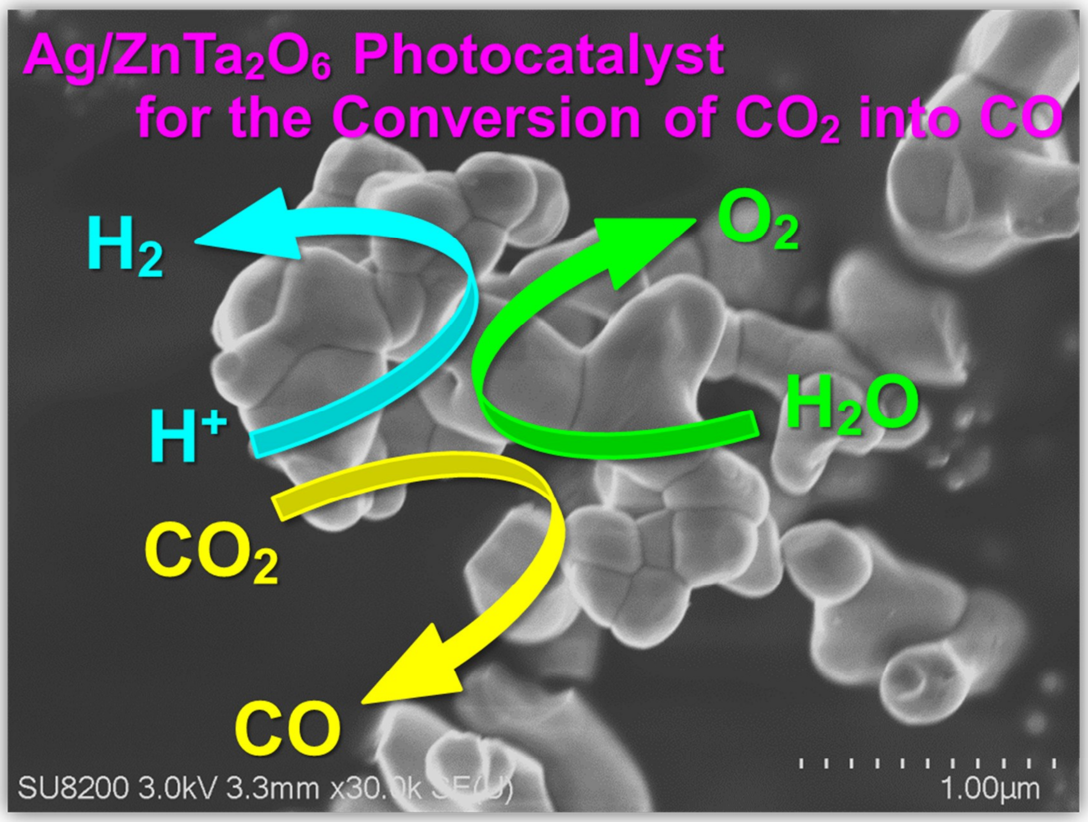

Textual abstract

Photocatalytic activity of $ZnTa_2O_6$ for the conversion of CO_2 using H_2O as a reductant was demonstrated. CO was produced as a reduction product of CO_2 in the presence of Ag cocatalyst, accompanied with the stoichiometric amount of O_2 evolution.